Physica A 525 (2019) 825–833

Contents lists available at ScienceDirect

Physica A

journal homepage: www.elsevier.com/locate/physa

Quantum metrology out of equilibrium

Sholeh Razavian [a], Matteo G.A. Paris [b,*]

[a] Faculty of Physics, Azarbaijan Shahid Madani University, Tabriz, Iran
[b] Quantum Technology Lab, Dipartimento di Fisica 'Aldo Pontremoli', Università degli Studi di Milano, I-20133 Milano, Italy

HIGHLIGHTS

- We suggest open quantum systems out-of-equilibrium as effective quantum probes.
- We establish a relationship between the QFI and the coherence of the probe.
- We suggest a scheme to estimate the ohmicity parameter of a bosonic environment.

ARTICLE INFO

Article history:
Received 6 December 2018
Received in revised form 2 March 2019
Available online 2 April 2019

Keywords:
Quantum probes
Complex systems
Ohmic reservoirs

ABSTRACT

We address open quantum systems out-of-equilibrium as effective quantum probes for the characterisation of their environment. We discuss estimation schemes for parameters driving a de-phasing evolution of the probe and then focus on qubits, establishing a relationship between the quantum Fisher information and the residual coherence of the probe. Finally, we apply our results to the characterisation of the ohmicity parameter of a bosonic environment.

1. Introduction

In this paper we address open quantum systems out-of-equilibrium [1,2], employed as quantum probes to precisely characterise some relevant properties of their environment [3–5]. The probing scheme we are going to discuss is the following (see Fig. 1): a quantum probe, i.e. a simple quantum system like a qubit, is prepared in a known initial state and then made to interact with a larger, and possibly complex, system, which represents the environment of the quantum probe. The environment usually induces decoherence, to an amount which depends on its temperature, spectral density and internal correlations [6]. The final state of the quantum probe thus carries information about the properties of the environment. In turn, any measurement performed on the probe may be exploited to infer the values of some relevant environment parameters [7–11]. In this situation, the inherent fragility of quantum systems to decoherence represents a resource, making quantum probes a very effective technique, able to provide enhanced precision compared to classical (thermal) probes [12,13]. In addition, quantum probes are usually *small* and do not perturb the system under investigation, thus representing a non-invasive technique suitable for delicate samples [14,15].

The interaction time between the probe and the system is usually a tunable parameter, and a question thus arises on whether it may be used to further optimise the estimation precision. In a classical setting, e.g. thermometry, this is not the case, since one prepares the probe, leave it interacting with the sample, and then read the environment parameter by measuring the probe when it has reached its stationary state, i.e. when it is at equilibrium with its environment. On the other hand, it has been recently shown that optimal estimation by quantum probes may be achieved also at finite

* Corresponding author.
E-mail address: matteo.paris@fisica.unimi.it (M.G.A. Paris).

https://doi.org/10.1016/j.physa.2019.03.125
0378-4371/

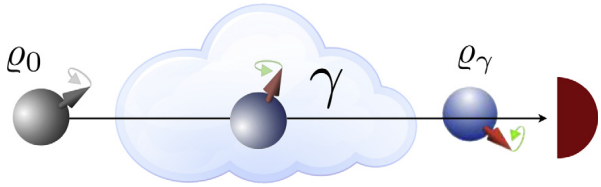

Fig. 1. A quantum probe is prepared in a known initial state and then made to interact with a larger, and possibly complex, system, which represents the environment of the probe itself. The final state of the quantum probes thus carries information about the properties of the environment, e.g. the parameter γ, which may be extracted by performing measurements at the output.

time, i.e. when the probe has not reached stationarity, and it is still in an out-of-equilibrium state [16–22]. Following this results, we address here open quantum systems out-of-equilibrium as possible quantum probes for the characterisation of their environment. At first, we discuss a general scheme to estimate parameters driving the de-phasing evolution of a probe. We then devote attention to qubit probes, and establish a relationship between the quantum Fisher information and the residual coherence of the probe. Finally, we apply our results to the estimation of the ohmicity parameter of a bosonic environment.

The paper is structured as follows. In Section 2, we establish notation, describe the dynamics of a probe subject to dephasing, and introduce the notion of residual coherence. In Section 3, we briefly review the tools of quantum parameter estimation. In Section 4, we address quantum probes out-of-equilibrium, establish a relationship between the quantum Fisher information and the residual coherence of the probe, and apply our results to the characterisation of the ohmicity parameter of a bosonic environment. Section 5 closes the paper with some concluding remarks.

2. Probing by dephasing

Let us consider a generic quantum system interacting with its environment. No assumptions is made on the dimension d of the Hilbert space of the probe. We also do not assume any specific form for the interaction Hamiltonian, but nevertheless assume that the resulting dynamics corresponds to a pure dephasing [23–26], i.e. to a Von Neumann–Liouville equation of the form

$$\dot{\varrho} = -i\,[H,\varrho] - \kappa\,[H,[H,\varrho]\,] \tag{1}$$

$$= -i\,[H,\varrho] + 2\,\kappa\,L[H]\,\varrho\,, \tag{2}$$

where ϱ is the density matrix describing the state of the system, H is its free Hamiltonian, $\kappa > 0$ is a dephasing rate and $L[O]\bullet = -\frac{1}{2}\{O^\dagger O,\bullet\} + O\bullet O^\dagger$ is a super-operator in the Lindblad form. Moving to the interaction picture, i.e. to a reference frame rotating with H, the equation of motion reduces to

$$\dot{\varrho} = 2\,\kappa\,L[H]\,\varrho\,. \tag{3}$$

Upon writing the initial state in the Hamiltonian basis, i.e. $\varrho_0 = \sum_{nk}\varrho_{nk}|e_n\rangle\langle e_k|$ with $H|e_n\rangle = E_n|e_n\rangle$, the state after the interaction with the environment is given by

$$\varrho_\gamma = \sum_{nk}\varrho_{nk}\,e^{-\gamma\,\Omega_{nk}^2}\,|e_n\rangle\langle e_k|\,, \tag{4}$$

$$= \int_{\mathbb{R}} dz\,g(z;0,2\gamma)\,e^{-izH}\varrho_0\,e^{izH} \tag{5}$$

where $\gamma = \kappa t$, $\Omega_{nk} = E_n - E_k$ and $g(z;\bar{z},\sigma^2)$ is a Gaussian distribution in the variable z with mean $\bar{z}$ and variance σ^2. The coherence of the probe after the interaction is given by

$$C_\gamma = \sum_{n\neq k}|\varrho_{nk}|\,e^{-\gamma\,\Omega_{nk}^2} = 2\sum_{n<k}|\varrho_{nk}|\,e^{-\gamma\,\Omega_{nk}^2}\,, \tag{6}$$

and is always smaller than the initial coherence $C_0 = 2\sum_{n<k}|\varrho_{nk}|$. Since the precision of quantum probes is strictly related to their sensitivity to decoherence, it is quite natural to start from a probe initially prepared in a maximally coherent state, i.e. $\varrho_0 = |\psi_0\rangle\langle\psi_0|$ where

$$|\psi_0\rangle = \frac{1}{\sqrt{d}}\sum_{nk}|e_n\rangle\langle e_k| \qquad C_0 = 1\,. \tag{7}$$

For the sake of simplicity we also assume equi-spaced levels for the probe, i.e. $\Omega_{nk}^2 = \Omega^2(n-k)^2$. In this case, the residual coherence after the interaction may be expressed as

$$C_\gamma = \frac{2}{d}\sum_{j=1}^{d-1} e^{-j^2\,\gamma\,\Omega^2}\,. \tag{8}$$

3. Quantum parameter estimation

After the interaction with the environment the state of the probe depends on the parameter we would like to estimate. In order to optimise the inference strategy, i.e. to optimise the extraction of information, we employ the tools of quantum estimation theory [27,28], which provides recipes to find the best detection scheme and to evaluate the corresponding lower bounds to precision. The precision also depends on the interaction time or, equivalently, on the residual coherence of the probe.

Let us consider the family of quantum states ρ_γ and assume that the dephasing rate depends on some parameter of interest, i.e. $\gamma = \gamma(\lambda)$. We perform measurements on repeated preparations of the probe and then process the overall sample of outcomes in order to estimate λ. Let us denote by Z the observable we measure on the probe ($Z|z\rangle = z|z\rangle$, $P_z = |z\rangle\langle z|$), and by $p(z|\lambda) = \mathrm{Tr}[\varrho_{\gamma(\lambda)} P_z]$ the distribution of its outcomes for a given value of λ. After choosing a certain observable Z, we perform M repeated measurements, collecting the data $\mathbf{z} = \{z_1, \ldots, z_M\}$. This set is then processed by an *estimator* $\widehat{\lambda} \equiv \widehat{\lambda}(\mathbf{z})$, i.e. a function from the space of data to the set of possible values of the parameter. The *estimate* value of the parameter is the mean value of the estimator over data, i.e.

$$\overline{\lambda} = \int d\mathbf{z}\, p(\mathbf{z}|\lambda)\widehat{\lambda}(\mathbf{z})\,, \tag{9}$$

where $p(\mathbf{z}|\lambda) = \Pi_{k=1}^{M} p(z_k|\lambda)$ since the repeated measurements are independent on each other. The *precision* of this estimation strategy corresponds to the variance of the estimator i.e.

$$V_\lambda \equiv \mathrm{Var}\,\lambda = \int d\mathbf{z}\, p(\mathbf{z}|\lambda)\left[\widehat{\lambda}(\mathbf{z}) - \overline{\lambda}\right]^2 . \tag{10}$$

The smaller is V_λ, the more precise is the estimation strategy. In fact, the precision of any unbiased estimator (i.e. an estimator such that $\overline{\lambda} \to \lambda$ for $M \gg 1$), is bounded by the so-called Cramèr–Rao (CR) inequality:

$$V_\lambda \geq \frac{1}{MF_\lambda} \tag{11}$$

where F_λ is the Fisher information (FI) of Z

$$F_\lambda = \int dz\, p(z|\lambda)\left[\partial_\lambda \log p(z|\lambda)\right]^2 , \tag{12}$$

i.e. the information that can be extracted on λ by performing measurements of Z on $\varrho_{\gamma(\lambda)}$. The best, i.e. more precise, measurement to infer the value of λ is the measurement maximising the FI, where the maximisation is performed over all the possible probe observables.

As a matter of fact, the maximum is achieved for any observable having the same spectral measure of the so-called *symmetric logarithmic derivative* L_λ, i.e. the selfadjoint operator satisfying the equation

$$2\,\partial_\lambda \varrho_{\gamma(\lambda)} = L_\lambda\, \varrho_{\gamma(\lambda)} + \varrho_{\gamma(\lambda)}\, L_\lambda\,. \tag{13}$$

The corresponding FI is usually referred to as the *quantum Fisher information* (QFI) and may be expressed as $H_\lambda = \mathrm{Tr}[\varrho_{\gamma(\lambda)} L_\lambda^2]$. Since $F_\lambda \leq H_\lambda$, the ultimate bound to precision in estimating λ by performing quantum measurements on $\varrho_{\gamma(\lambda)}$ is given by the quantum CR bound

$$V_\lambda \geq \frac{1}{MH_\lambda}\,. \tag{14}$$

In terms of the eigenvalues and eigenvectors of $\varrho_\gamma = \sum_n \varrho_n |\phi_n\rangle\langle\phi_n|$ the QFI may be written as

$$H_\lambda = \sum_n \frac{(\partial_\lambda \varrho_n)^2}{\varrho_n} + 2\sum_{n\neq k} \frac{(\varrho_n - \varrho_k)^2}{\varrho_n + \varrho_k}\left|\langle\phi_k|\partial_\lambda\phi_n\rangle\right|^2 . \tag{15}$$

In order to evaluate analytically the QFI, we need to diagonalise the density matrix of the probe after the interaction, i.e. that in Eq. (4). This can be done easily for low dimensional probes (qubit and qutrits), whereas numerical solutions are often needed for higher dimensions [29]. Upon maximising the QFI one then optimises the estimation scheme [30,31].

A global measure of the estimability of a parameter, which compares the variance with the value of the parameter, is given by the signal-to-noise ratio $R_\lambda = \lambda^2/V_\lambda$. In turn, the quantum CR bound may be rewritten in terms of R_λ as follows

$$R_\lambda \leq Q_\lambda = \lambda^2 H_\lambda\,, \tag{16}$$

where Q_λ is referred to as the quantum signal-to-noise ratio (QSNR).

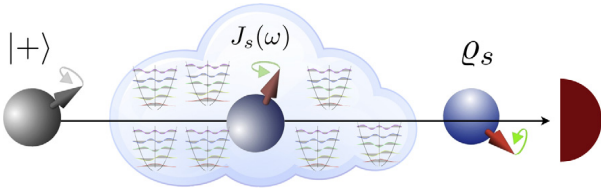

Fig. 2. A qubit is prepared in a maximally coherent state $|+\rangle = (|e_1\rangle + |e_2\rangle)/\sqrt{2}$ and then is made to interact with a Ohmic-like environment made of bosonic modes, characterised by a spectral density $J_s(\omega)$ The output state of the probe carries information about the ohmicity parameter s, which may be estimated by performing measurements at the output.

4. Quantum probes out of equilibrium

Let us now consider the simplest quantum probe, i.e. a qubit system used to characterise its environment, which itself induces dephasing on the qubit. In this case we may consider a generic pure initial state $|\psi_0\rangle = \cos\phi|e_1\rangle + \sin\phi|e_2\rangle$ and use the notation $\Omega = \Omega_{21} = E_2 - E_1$. The initial coherence is given by $C_0 = \sin 2\phi$ and the final one by $C_\lambda \equiv C_{\gamma(\lambda)} = e^{-\gamma(\lambda)\Omega^2}\sin 2\phi$. In order to evaluate the QFI, we leave the qubit to evolve, then diagonalise the state, and finally use Eq. (15). After some algebra, we obtain a remarkably compact formula

$$H_\lambda = \Omega^4 \left(\partial_\lambda \gamma\right)^2 \frac{C_0^2 C_\lambda^2}{C_0^2 - C_\lambda^2}\,, \tag{17}$$

which is valid for any ϕ and expresses the QFI in terms of the dependence of the dephasing rate on the parameter of interest, i.e. the *susceptibility* $\partial_\lambda\gamma$, and on the relationship between the initial and the final coherence of the probe. As it may easily proved, the maximum of the QFI is achieved for $\phi = \pi/4$, thus confirming the intuition, already mentioned in Section 2, that the optimal initial state of the probe corresponds to a maximally coherent state $|+\rangle = (|e_1\rangle + |e_2\rangle)/\sqrt{2}$. We remark that Eq. (17) is valid for any (pure) initial preparation of the probe and any kind of parameter, the only assumption being that the preparation of the environment and the corresponding interaction leads to a pure dephasing evolution of the probe .

As an application, let us now consider a qubit, used to probe the nature of an Ohmic-like environment made of bosonic modes (see Fig. 2). In order to introduce the problem, let us write the Hamiltonian of the whole system. We use the natural system of units ($\hbar = 1$), and also write the Hamiltonian in unit of the qubit frequency Ω, making it adimensional

$$\mathcal{H} = \frac{1}{2}\sigma_3 + \sum_k \omega_k\, b_k^\dagger\, b_k + \sigma_3 \sum_k (g_k\, b_k^\dagger + g_k^*\, b_k)\,, \tag{18}$$

where ω_k is the (dimensionless) frequency of the kth environmental mode. The σ's are the Pauli matrices and $[b_k, b_k^\dagger] = \delta_{kk'}$ describe the modes of the environment. The g_k's are coupling constants, describing the interaction of each mode with the qubit probe. Their distribution determines the *spectral density* of the environment, according to the expression $J(\omega) = \sum_k |g_k|^2\,\delta(\omega_k - \omega)$. The spectral density is the crucial quantity to describe the system-environment interaction, and it does depend on the specific features of the environment. In turn, the characterisation of the spectral density is crucial to understand, and possibly control, quantum decoherence [32–37].

A large class of structured reservoirs is characterised by an *Ohmic*-like spectral density of the form

$$J_s(\omega) = \omega_c \left(\frac{\omega}{\omega_c}\right)^s \exp\left\{-\frac{\omega}{\omega_c}\right\}\,, \tag{19}$$

where the frequencies are in unit of Ω. The cutoff frequency describes a natural boundary in frequency response of the system. As we will see, it determines the timescale of the evolution. The quantity s is a real positive number, which governs the behaviour of the spectral density at low frequencies. Upon varying s we move from the so-called sub-Ohmic regime ($s < 1$), to Ohmic ($s = 1$), and to super-Ohmic one ($s > 1$). Different values of the ohmicity parameter s often correspond to radically different kinds of dynamics, and therefore it would be highly desirable to have an estimation scheme for their precise characterisation.

Such a scheme may be obtained from the results of the previous Sections, since the dynamics induced on the qubit is a pure dephasing. In order to prove this result, one assumes that the system is initially in the state $|\psi\rangle \otimes |0\rangle$ (i.e. a generic state for the probe and, assuming to be at zero temperature, the ground state for the environment), then evolve the whole system according to the Hamiltonian in Eq. (18), and finally trace out the environment. The resulting evolution is that of Eq. (4) where the dephasing rate is given by

$$\gamma_s(\tau) = \int_0^\infty \frac{1 - \cos(\omega\tau/\omega_c)}{\omega^2} J_s(\omega)\, d\omega\,, \tag{20}$$

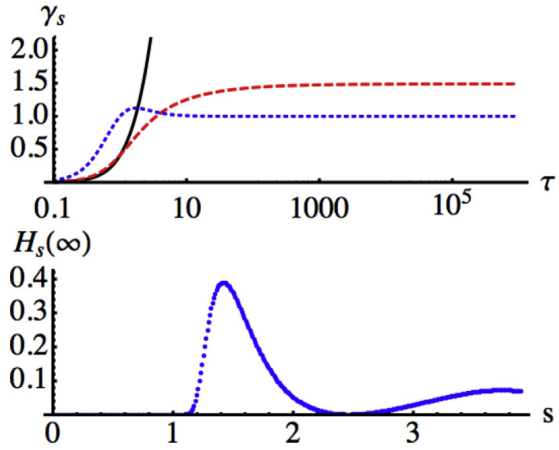

Fig. 3. (Top): the dephasing rate $\gamma_s(\tau)$ as a function of τ for three values of $s = 0.1$ (solid black line), 1.6 (dashed red line), and 3.0 (dotted blue line). (Bottom): the asymptotic value $H_s(\infty)$ of the QFI as a function of the ohmicity parameter s. We have $H_s(\infty) = 0$ for $s \leq 1$, and $H_s(\infty) \neq 0$ for $s > 1$.

$$= \begin{cases} \frac{1}{2}\log\left(1+\tau^2\right) & s = 1 \\ \left(1 - \frac{\cos\left[(s-1)\arctan\tau\right]}{\left(1+\tau^2\right)^{\frac{s-1}{2}}}\right)\Gamma[s-1] & s \neq 1 \end{cases} \tag{21}$$

where $\tau = \omega_c t$ and $\Gamma[x] = \int_0^\infty t^{x-1}e^{-t}dt$ is the Euler Gamma function. For short time we have $\gamma_s(\tau) \simeq \frac{1}{2}\tau^2\Gamma[1+s]$ $\forall s$, whereas for large value of τ the dephasing rate diverges for $s \leq 1$, and shows a finite asymptotic value $\gamma_s(\infty) = \Gamma[s-1]$ for $s > 1$. In the upper panel of Fig. 3, we show the behaviour of $\gamma_s(\tau)$ as a function of τ for three different values of s.

Upon preparing the qubit in the initial state $|+\rangle = (|0\rangle + |1\rangle)/\sqrt{2}$, the evolved state $\varrho_s^+(\tau)$ is obtained from Eqs. (4) and (21). Then, using Eq. (17) the QFI for the estimation of s is given by

$$H_s(\tau) = \frac{\left[\partial_s\gamma_s(\tau)\right]^2}{e^{2\gamma_s(\tau)} - 1}\,, \tag{22}$$

where the interaction time τ is a free parameter that can be used to further optimise precision. Notice that the short-time behaviour of $H_s(\tau)$, as well as the asymptotic one, may be extracted from the corresponding behaviour of the dephasing rate $\gamma_s(\tau)$. For short time we have $H_s(\tau) \simeq \tau^2 g_s$, where

$$g_s = \frac{\Gamma[s-1]}{4s(s-1)}\left(2s - 1 + s(s-1)\psi[s-1]\right)^2\,,$$

$\psi[z] = \Gamma'[z]/\Gamma[z]$ being the logarithmic derivative of the gamma function. For large value of τ we have $H_s(\infty) = 0$ for $s \leq 1$, and $H_s(\infty) \neq 0$ for $s > 1$. The behaviour of the asymptotic value $H_s(\infty)$ as a function of the ohmicity parameter is illustrated and summarised in the lower panel of Fig. 3.

In Fig. 4 we show the behaviour of H_s as a function of s and τ. In order to emphasise the non trivial features of this function, we first show a 2D plot as a function of time for three values of s (upper panel), a 3D plot illustrating the behaviour for limited interaction time ($\tau \leq 7$, middle left plot) and a contour plot with a longer time range ($\tau \leq 35$, middle right plot). In order to optimise the estimation of s we should chose the interaction time that maximises the QFI. As it may be guessed from the plots, this optimal time τ_s increases with s when s is small, and then jump to a smaller value for larger values of s. We obtain numerically the following estimate $\tau_s \simeq \pi e^s/2$ for $s \ll 1$ and $\tau_s = \pi/(2s)$ for $2.2 \lesssim s \lesssim 3$. In the intermediate region, H_s is an increasing (though saturating) function of τ, and the optimal strategy would be to leave the qubit interacting with the environment as much as it can. Of course, this is not possible, due to the finite size of any environment. Thus the prescription is that of choosing a generically *large* interaction time. Overall, we have that depending on the values of s, one may achieve optimal estimation at finite interaction time (i.e. out-of-equilibrium) or for large time (when, presumably, the qubit has reached its stationary state [38]). The behaviour of τ_s as a function of s is shown in the lower panel of Fig. 4. Our results confirm that pure dephasing is an effective mechanism to gain information about the system under investigation without exchanging energy.

In the upper panel of Fig. 5 we show the optimised value of H_s as a function of s, whereas in the lower panel we show the corresponding quantum signal-to-noise ratio $Q_s = s^2 H_s$. The physical meaning of these plots is that estimation of intermediate values of s, corresponding to slightly super-Ohmic environments ($s \simeq 1.5$), is inherently more precise than the estimation of smaller or slightly larger values ($1.5 \lesssim s \lesssim 2.5$).

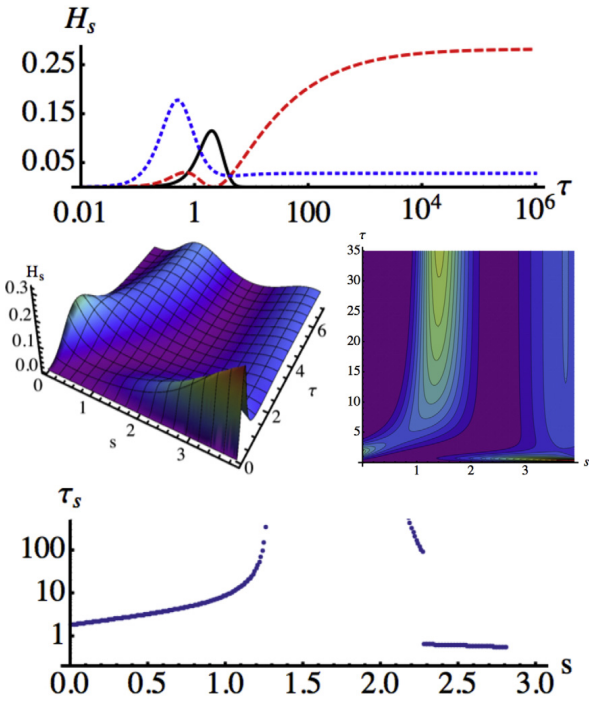

Fig. 4. (Top): The QFI H_s as a function of τ for three values of $s = 0.1$ (solid black line), 1.6 (dashed red line), and 3.0 (dotted blue line). (Middle): The QFI H_s as a function of s and τ. On the left a 3D plot for interaction times $\tau \leq 7$, and on the right a contour plot illustrating the behaviour for a longer time range ($\tau \leq 35$). (Bottom): The time value τ_s, maximising H_s at fixed s. The value τ_s increases with s when s is small and then jump to a smaller value for larger values of s. In the intermediate region, H_s is an increasing function of τ.

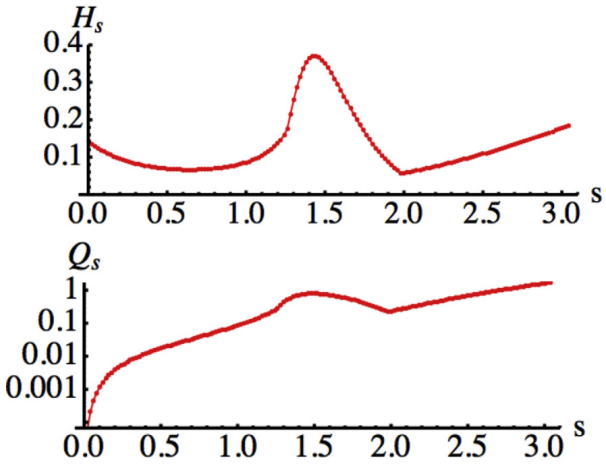

Fig. 5. (Top): The optimal value QFI H_s, maximised over τ, as a function of s. (Bottom): the corresponding quantum signal-to-noise ratio Q_s. As it is apparent from the plots, estimation of intermediate values of s, corresponding to slightly super-Ohmic environments ($s \simeq 1.5$), is inherently more precise than the estimation of smaller values, and also of slightly larger values.

4.1. Feasible measurement achieving optimal precision

In this Section we discuss the feasibility of the optimal measurement, i.e. whether it exists a measurement for which the associated Fisher information is equal to the QFI. To this aim, let us consider the most general projective measurement $\{P_\pm\}$, $P_+ + P_- = \mathbb{I}$ on the qubit probe, i.e.

$$P_\pm = \frac{\mathbb{I} \pm \boldsymbol{b} \cdot \boldsymbol{\sigma}}{2}\,, \tag{23}$$

where $\boldsymbol{b} = (b_1, b_2, b_3)$, $|\boldsymbol{b}| = 1$ and $\boldsymbol{\sigma}$ is the vector of the Pauli matrices, $\sigma_x, \sigma_y, \sigma_z$. The probability distribution of the two outcomes for the qubit probe initially prepared in the state $|+\rangle$ is given by

$$p_{\pm}(\tau) = \mathrm{Tr}\left[\varrho_s^{+}(\tau) P_{\pm}\right] = \frac{1}{2}\left[1 \pm b_1 e^{-\gamma_s(\tau)}\right], \tag{24}$$

corresponding to a Fisher information

$$F_s = \sum_{k=\pm} \frac{[\partial_s p_k(\tau)]^2}{p_k(\tau)}. \tag{25}$$

Starting from the above equation, it is easy to see that we have $F_s = H_s$ if $b_1 = 1$, i.e. for the measurement of σ_x on the qubit. This means that measuring σ_x provides optimal estimation of the parameter s, provided that an efficient estimator is employed to process the data. The overall optimal strategy thus consists in the preparation of the qubit in an eigenstate of σ_x and the measurement of the same observable after the interaction with the environment.

4.2. Quantum probes at nonzero temperature

If temperature T of the environment is not strictly zero, the dephasing rate is given by

$$\gamma_s(\tau, T) = \int_0^{\infty} d\omega \, \frac{1 - \cos(\omega\tau/\omega_c)}{\omega^2} J_s(\omega) \coth\frac{\omega}{2T}, \tag{26}$$

which is usually hard to evaluate analytically for a generic value of s. In many situation of interest, however, the temperature is not too high and we may use the approximate expression

$$\coth\frac{\omega}{2T} \overset{T\ll 1}{\simeq} 1 + 2e^{-\omega/T}.$$

In those situations, the dephasing rate may be written as

$$\gamma_s(\tau, T) \simeq \gamma_s(\tau, 0) + 2\left(\frac{1+T}{T}\right)^{1-s} \gamma_s\left(\frac{T\tau}{1+T}, 0\right) \tag{27}$$

$$\simeq \gamma_s(\tau, 0) + \frac{T^{1+s}(1-T)}{(1+T)^s} \tau^2 \Gamma[1+s], \tag{28}$$

where $\gamma_s(\tau, 0)$ is given in Eq. (21), and temperature is an adimensional quantity, expressed in unit of ω_c [39]. Using Eq. (28), an analytic expression for the QFI H_s at low temperature may be obtained and compared with the zero temperature case. In order to quantify the effects of temperature we introduce the excess QFI

$$\Delta H_s(\tau, T) = H_s(\tau, T) - H_s(\tau, T \equiv 0), \tag{29}$$

which is positive when a nonzero temperature leads to an improvement in precision, and negative otherwise. In Fig. 6 we show the absolute value $|\Delta H_s(\tau, T)|$ of the excess QFI as a function of s and τ for two different values of the temperature. On the left we show the function for $T = \omega_c/100$ and on the right for $T = \omega_c/10$. The blue region corresponds to $\Delta H_s(\tau, T) > 0$, i.e. working at nonzero temperature is convenient in terms of the achievable precision, and the green one to $\Delta H_s(\tau, T) < 0$, i.e. regions where temperature is degrading performances. Upon looking at Fig. 6 and noticing the different scale with respect to Fig. 4b, one concludes that (low) temperature has only a minor effect on the achievable precision. Accordingly, the optimal interaction time for the probe, and the resulting maximum value of the QFI are only slightly changed. In the opposite limit, i.e. when the temperature is high, the situation dramatically changes. This may be easily seen by expanding the hyperbolic cotangent as $\coth x \simeq x^{-1}$, thus arriving at

$$\gamma_s(\tau, T) \simeq \frac{1}{2T} \gamma_{1+s}(\tau, 0).$$

Moreover, since $\gamma_{1+s}(\tau, 0)$ is a bounded function of τ, we have

$$H_s(\tau, T) = \frac{1}{4T^2} \frac{\left[\partial_s \gamma_{1+s}(\tau, 0)\right]^2}{e^{\gamma_{1+s}(\tau,0)/T} - 1}$$

$$\approx \frac{1}{T} H_{1+s}(\tau, 0). \tag{30}$$

Eq. (30) says that the QFI for the ohmicity parameter at high temperature is largely reduced in comparison to the low temperature case, i.e. almost no information may be extracted by quantum probes. Indeed, this is matching physical intuition, since for large temperature decoherence is mostly due to thermal fluctuations rather than the specific features of the interaction, and thus the probes is unable to extract information about the structure of the environment.

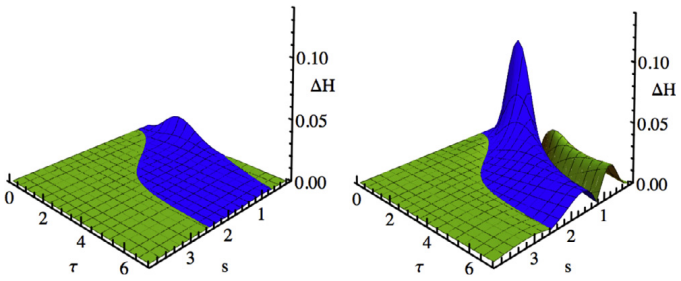

Fig. 6. The absolute value $|\Delta H_s(\tau, T)|$ of the excess QFI as a function of s and τ for two different values of the temperature. On the left the function for $T = \omega_c/100$ and on the right for $T = \omega_c/10$. The blue region corresponds to $\Delta H_s(\tau, T) > 0$ and the green one to $\Delta H_s(\tau, T) < 0$. Notice the different scale with respect to Fig. 4b.

5. Conclusions

In this paper we have addressed the use of open quantum systems out-of-equilibrium as possible quantum probes for the characterisation of their environment. In particular, we have discussed estimation schemes involving parameters governing a de-phasing evolution of the probe. For qubit probe we have found a simple relation linking the quantum Fisher information to the residual coherence of the probe. Finally, we have addressed in some details the estimation of the ohmicity parameter of a bosonic environment, finding that depending on the values of s, one may achieve optimal estimation at finite interaction time, i.e. when the probe is in an out-of-equilibrium state, or for large time, when, presumably, the qubit has reached its stationary state. Overall, our results pave the way for further investigation about out-of-equilibrium quantum metrology, perhaps exploiting memory effects [40], and confirm that pure dephasing at low temperature represents an effective mechanism to imprint information on quantum probes without exchanging energy with the system under investigation.

Acknowledgments

This work has been supported by CARIPLO foundation (Italy) through the Lake-of-Como School program, and by SERB (India) through the VAJRA scheme (grant VJR/2017/000011). MGAP is member of GNFM-INdAM. The authors are grateful to Matteo Bina, Claudia Benedetti, and Luigi Seveso, for useful discussions.

References

[1] G. Schaller, Open Quantum Systems Far From Equilibrium, in: Lect. Not. Phys., vol. 881, Springer, Berlin, 2014.
[2] H.-P. Breuer, F. Petruccione, The Theory of Open Quantum Systems, Oxford University Press, 2009.
[3] T.J. Elliott, T.H. Johnson, Nondestructive probing of means, variances, and correlations of ultracold-atomic-system densities via qubit impurities, Phys. Rev. A 93 (2016) 043612.
[4] M. Streif, A. Buchleitner, D. Jaksch, J. Mur-Petit, Measuring correlations of cold-atom systems using multiple quantum probes, Phys. Rev. A 94 (2016) 053634.
[5] F. Cosco, M. Borrelli, F. Plastina, S. Maniscalco, Momentum-resolved and correlation spectroscopy using quantum probes, Phys. Rev. A 95 (2017) 053620.
[6] M. Palma, K.-A. Suominen, A.K. Ekert, Quantum computers and dissipation, Proc. R. Soc. London Ser. A 452 (1996) 567.
[7] C. Benedetti, M.G.A. Paris, Characterization of classical Gaussian processes using quantum probes, Phys. Lett. A 378 (2014) 2495.
[8] M.G.A. Paris, Quantum probes for fractional Gaussian processes, Physica A 413 (2014) 256.
[9] A. Zwick, G.A. Alvarez, G. Kurizki, Maximizing information on the environment by dynamically controlled qubit probes, Phys. Rev. Appl. 5 (2016) 014007.
[10] A. Fujiwara, H. Imai, Quantum parameter estimation of a generalized Pauli channel, J. Phys. A: Math. Gen. 36 (2003) 8093.
[11] O. Pinel, P. Jian, N. Treps, C. Fabre, D. Braun, Quantum parameter estimation using general single-mode Gaussian states, Phys. Rev. A 88 (2013) 040102(R).
[12] M. Brunelli, S. Olivares, M.G.A. Paris, Qubit thermometry for micromechanical resonators, Phys. Rev. A 84 (2011) 032105.
[13] M. Brunelli, S. Olivares, M. Paternostro, M.G.A. Paris, Qubit-assisted thermometry of a quantum harmonic oscillator, Phys. Rev. A 86 (2012) 012125.
[14] J. Gemmer, M. Michel, G. Mahler, Quantum Thermodynamics, in: Lect. Not. Phys, vol. 784, Springer, Berlin, 2004.
[15] M. Horodecki, J. Oppenheim, Fundamental limitation for quantum and nano-scale thermometry, Nat. Comm. 4 (2013) 2059.
[16] C. Invernizzi, M. Korbmann, L. Campos-Venuti, M.G.A. Paris, Optimal quantum estimation in interacting spin systems, Phys. Rev. A 78 (2008) 042106.
[17] U. Marzolino, T. Prosen, Quantum metrology with non-equilibrium steady states of quantum spin chains, Phys. Rev. A 90 (2014) 062130.
[18] V. Cavina, et al., Bridging thermodynamics and metrology in non-equilibrium Quantum Thermometry, Phys. Rev. A 98 (2018) 050101.
[19] Z. Wang, W. Wu, G. Cui, J. Wang, Coherence enhanced quantum metrology in a nonequilibrium optical molecule, New J. Phys. 20 (2018) 033034.
[20] L.A. Correa, M. Mehboudi, G. Adesso, A. Sanpera, Individual quantum probes for optimal thermometry, Phys. Rev. Lett. 114 (2015) 220405.
[21] S. Jevtic, D. Newman, T. Rudolph, T.M. Stace, Single-qubit thermometry, Phys. Rev. A 91 (2015) 012331.
[22] S. Campbell, M.G. Genoni, S. Deffner, Precision thermometry and the quantum speed limit, Quantum Sci. Technol. 3 (2018) 025002.
[23] Sh. Razavian, C. Benedetti, M. Bina, Y. Akbari-Kourbolagh, M.G.A. Paris, Quantum thermometry by single-qubit dephasing, arXiv:1807.11810.

[24] C. Benedetti, M.G.A. Paris, Effective dephasing for a qubit interacting with a transverse classical field, Int. J. Quantum Inf. 12 (2014) 1461004.
[25] M.A.C. Rossi, et al., Engineering decoherence for two-qubit systems interacting with a classical environment, Int. J. Quantum Inf. 12 (2014) 1560003.
[26] C. Addis, G. Brebner, P. Haikka, S. Maniscalco, Coherence trapping and information backflow in dephasing qubits, Phys. Rev. A 89 (2014) 024101.
[27] C.W. Helstrom, Quantum Detection and Estimation Theory, Academic Press, 1976.
[28] M.G.A. Paris, Quantum estimation for quantum technology, Int. J. Quantum Inf. 7 (2009) 125.
[29] J. Liu, H.-N. Xiong, F. Song, X. Wang, Fidelity susceptibility and quantum fisher information for density operators with arbitrary ranks, Physica A 410 (2014) 167.
[30] C. Cafaro, S. Mancini, On grover search algorithm from a quantum information geometry viewpoint, Physica A 391 (2012) 1610.
[31] J. He, Z.-Y. Ding, L. Yeb, Enhancing quantum fisher information by utilizing uncollapsing measurements, Physica A 457 (2016) 598.
[32] J. Paavola, J. Piilo, K.-A. Suominen, S. Maniscalco, Environment-dependent dissipation in quantum Brownian motion, Phys. Rev. A 79 (2009) 052120.
[33] R. Martinazzo, K.H. Hughes, F. Martelli, I. Burghardt, Effective spectral densities for system-environment dynamics at conical intersections: S2-S1 conical intersection in pyrazine, Chem. Phys. 377 (2010) 21.
[34] C.J. Myatt, et al., Decoherence of quantum superpositions through coupling to engineered reservoirs, Nature 403 (2000) 269.
[35] J. Piilo, S. Maniscalco, Driven harmonic oscillator as a quantum simulator for open systems, Phys. Rev. A 74 (2006) 032303.
[36] M. Bina, F. Grasselli, M.G.A. Paris, Continuous-variable quantum probes for structured environments, Phys. Rev. A 97 (2018) 012125.
[37] C. Benedetti, F. Salary, M.H. Zandi, M.G.A. Paris, Quantum probes for the cutoff frequency of Ohmic environments, Phys. Rev. A 97 (2018) 012126.
[38] F. Troiani, M.G.A. Paris, Universal quantum magnetometry with spin states at equilibrium, Phys. Rev. Lett. 120 (2018) 260503.
[39] More generally, upon expanding the hyperbolic cotangent as $\coth x = (1+e^{-2x})\sum_{n=0}^{\infty} e^{-2nx}$, we obtain

$$\gamma_s(\tau, T) = \gamma_s(\tau, 0) + 2\sum_{n=0}^{\infty} a_n^{1-s}\,\gamma_s\left(\frac{\tau}{a_n}, 0\right),$$

where

$$a_n \equiv a_n(T) = 1 + \frac{n}{T},$$

with τ and T expressed in unit of ω_c.
[40] C. Benedetti, M.G.A. Paris, S. Maniscalco, Non-Markovianity of colored noisy channels, Phys. Rev. A 89 (2014) 012114.